Biochemical and Biophysical Research Communications 406 (2011) 366–370

Contents lists available at ScienceDirect

Biochemical and Biophysical Research Communications

journal homepage: www.elsevier.com/locate/ybbrc

Redox-active tyrosine residue in the microcin J25 molecule

Miriam C. Chalón [a], Natalia Wilke [b], Jens Pedersen [c], Stefano Rufini [c], Roberto D. Morero [a], Leonardo Cortez [a], Rosana N. Chehín [a], Ricardo N. Farias [a], Paula A. Vincent [a,*]

[a] Departamento de Bioquímica de la Nutrición, Instituto Superior de Investigaciones Biológicas (Consejo Nacional de Investigaciones Científicas y Técnicas-Universidad Nacional de Tucumán) and Instituto de Química Biológica "Dr Bernabé Bloj", Chacabuco 461, 4000 San Miguel de Tucumán, Tucumán, Argentina
[b] CIQUIBIC, Dpto. de Química Biológica, Facultad de Ciencias Químicas, Universidad Nacional de Córdoba, Pabellón Argentina, Ciudad Universitaria, X5000HUA, Córdoba, Argentina
[c] Department of Biology, University of Rome Tor Vergata 00133, Rome, Italy

ARTICLE INFO

Article history:
Received 21 January 2011
Available online 15 February 2011

Keywords:
Tyrosyl radical
Redox peptide
EPR

ABSTRACT

Microcin J25 (MccJ25) is a 21 amino acid lasso-peptide antibiotic produced by *Escherichia coli* and composed of an 8-residues ring and a terminal 'tail' passing through the ring. We have previously reported two cellular targets for this antibiotic, bacterial RNA polymerase and the membrane respiratory chain, and shown that Tyr9 is essential for the effect on the membrane respiratory chain which leads to superoxide overproduction. In the present paper we investigated the redox behavior of MccJ25 and the mutant MccJ25 (Y9F). Cyclic voltammetry measurements showed irreversible oxidation of both Tyr9 and Tyr20 in MccJ25, but infrared spectroscopy studies demonstrated that only Tyr9 could be deprotonated upon chemical oxidation in solution. Formation of a long-lived tyrosyl radical in the native MccJ25 oxidized by H_2O_2 was demonstrated by Electron Paramagnetic Resonance Spectroscopy; this radical was not detected when the reaction was carried out with the MccJ25 (Y9F) mutant. These results show that the essential Tyr9, but not Tyr20, can be easily oxidized and form a tyrosyl radical.

1. Introduction

Redox-active tyrosine residues play important roles in catalysis in several enzymes, including ribonucleotide reductase, prostaglandin H synthase, and photosystem II. Oxidation of tyrosine or tyrosinate results in the production of a tyrosyl radical. In these enzymes, tyrosyl radicals are proposed to act as intermediaries in long-distance electron transfer reactions [1]. The environmental factors responsible for functional control of these redox-active species have not yet been elucidated [2]. Vassiliev et al. [3] showed that the primary structure influences the functional properties of redox-active tyrosines in ribonucleotide reductase and photosystem II enzymes.

The MccJ25 is a plasmid-encoded 21 amino acid antibiotic peptide produced by *Escherichia coli* (*E. coli*) and active against *E. coli, Salmonella* and *Shigella* strains [4–6]. The peptide has a lasso-structure that contains a lactam linkage between the α-amino group of Gly1 and the γ-carboxyl of Glu8, forming an eight-residue ring (Gly1–Glu8), which is termed a lariat ring. The 'tail' (Tyr9-Gly21) passes through the ring, with Phe19 and Tyr20 straddling each side of the tail, sterically trapping the tail within the ring [7–9].

Convincing evidences showing that RNA polymerase (RNAP) is the target for MccJ25 action in *E. coli* were previously provided by our laboratory. The peptide inhibits the enzyme activity by obstructing the secondary channel and consequently preventing access of the substrates to its active sites [10–13]. MccJ25 also targets the respiratory chain enzymes of the bacterial membrane with the consequent inhibition of cell oxygen consumption [14,15]. This effect is mediated by an increase in superoxide production during the membrane respiratory processes [16].

We recently demonstrated that only Tyr9 of MccJ25 is responsible of the peptide effect on membrane respiratory chain in *E. coli* [17]. A single Y9F mutation abolishes superoxide overproduction and oxygen consumption inhibition induced by the antibiotic, strongly suggesting that Tyr9 is involved in the MccJ25 action on the respiratory chain of *E. coli*. Taking into account this previous result and the importance of redox-active tyrosines in several enzymes, appears as fundamental the need to study the redox properties of the MccJ25 which could give information to elucidate the antibiotic mechanism on cell membrane.

In the present paper, the formal redox potential of MccJ25 was estimated by cyclic voltammetry. We demonstrated that the two tyrosines (Tyr9 and Tyr20) of the antibiotic molecule were able to

Abbreviations: MccJ25, Microcin J25; RNAP, RNA polymerase; DBNBS, dibromo-4-nitrosobenzenesulfonate; DMPO, 5,5-dimethylpyrroline-N-oxide; MNP, 2-methyl-2-nitrosopropane; EPR, Electronic Paramagnetic Resonance; TFA, trifluoracetic acid; *E*p, peak potential value; log *v*, logarithmic of the sweep rate; metMb, metmyoglobin.

* Corresponding author. Address: Departamento de Bioquímica de la Nutrición, INSIBIO, Chacabuco 461, CP: 4000, San Miguel de Tucumán, Argentina. Fax: +54 54 381 4248921.
E-mail address: pvincent@fbqf.unt.edu.ar (P.A. Vincent).

0006-291X/$ - see front matter © 2011 Elsevier Inc. All rights reserved.
doi:10.1016/j.bbrc.2011.02.047

participate of an irreversible oxidation process, however only the Tyr9 can contribute in the oxidative redox reaction in homogeneous phase. Moreover, the presence of a MccJ25 tyrosyl radical was confirmed by Electronic Paramagnetic Resonance (EPR) method.

2. Materials and methods

2.1. Isolation of MccJ25 and MccJ25 (Y9F) peptides

MccJ25 was purified from 2-liter cultures of strain MC4100 harboring pTUC202 as previously described [14]. The isolation of mutant peptide MccJ25 (Y9F) was performed as described by Chalón et al. [17]. Native MccJ25 and MccJ25 (Y9F) were purified by HPLC, as described previously [14].

2.2. Cyclic voltammetry

Cyclic voltammetry was performed using an Autolab electrochemical analyzer GPSTAT30. The electrochemical measurements were carried out in a three-electrode conventional cell. The counter electrode was a glassy carbon rod of greater area than the working electrode and the reference electrode was satured calomel. All the informed potentials are referred to the standard hydrogen electrode potential considering a potential difference of 0.241 V between saturated calomel and standard hydrogen electrodes. A hanging mercury drop electrode (VA 663 Methrom, Switzerland) was used as the working electrode (0.0025 cm^2 of area). All the experiments were performed in a 50 mM phosphate buffer solution at pH 7, applying an initially anodic potential sweep from 0 to 1.7 V at different scan rates. The cell was purged before each cyclic with N_2 for 5 min. The peptide concentration was 20 μM.

2.3. Fourier transform infrared (FTIR) spectroscopy

The infrared spectra of the peptides were analyzed in the absence and in the presence of 300 mM $K_3[Fe_6]$ in 40 mM buffer HEPES-D_2O, pD 7.4 (pD = pH + 0.4 pH unit), with previous trifluoracetic acid (TFA) removal according to Gaussier et al. [18]. In all cases, the peptide concentration was 2.4 mM. The samples were loaded onto a demountable liquid cell (Harrick Scientific, Ossining, NY) with calcium fluoride windows with 100 μm spacers. The samples were recorded in a Nicolet 5700 spectrometer equipped with a DTGS detector (Thermo Nicolet, Madison, WI). The sample chamber was purged with dry, CO_2-free air. Spectra were collected by using OMNIC (Nicolet) software. Usually, 256 scans/samples were taken, averaged, apodized with a Happ-Genzel function, and Fourier transformed to give a final resolution of 1 cm^{-1}. The contribution of D_2O in the amide I region was eliminated by subtracting the buffer spectra from that of the solution at the same temperature to obtain a flat baseline of between 2000 and 1700 cm^{-1}. Peptide amide I analyses either in the absence or in the presence of ferricyanide were repeated three times with fresh new samples to test the reproducibility of the measurements. In all cases, the differences among the three experiments were lower than 2%. The spectra deconvolution and band position determination were performed by using NRC software (Canadian National Research Council). In order to increase the spectral resolution, 2D heterospectral correlation analysis was performed between normalized spectra with and without ferricyanide addition. To obtain the 2D-IR maps, the presence of ferrycianide was used as the perturbation to induce spectral fluctuations and to detect dynamic spectral variations on the secondary structure of the peptides. The two-dimensional synchronous map was obtained correlating the normalized spectra by using software with the algorithm previously described by Turnay et al. [19].

2.4. EPR experiments

Incubations consisting of 2.4 mM MccJ25 or MccJ25 (Y9F) peptides and 1 mM 3,5-Dibromo-4-nitrosobenzenesulfonate (DBNBS) in 50 mM sodium borate buffer, pH 10 were rapidly mixed with 2.5 mM H_2O_2. Samples were subsequently transferred to a 100 μl capillary tube and EPR measurements were made at room temperature (22–25 °C) with a Bruker ESP300 X-band instrument (Bruker, Karlsruhe, Germany) equipped with a high sensitivity TM110-mode cavity. Spectra were measured over a 20 G range using 40 milliwatts power, 2.6 G modulation, 1×10^5 receiver gain, and a scan time of 30 min; typically 40 single scans were accumulated to improve the signal to noise ratio.

3. Results and discussion

3.1. Cyclic voltammetry

Fig. 1 shows representative cyclic voltammogram profiles obtained at different sweep rates for solutions with 20 μM of MccJ25 in phosphate buffer at pH 7. The assay was performed also with a mutant peptide MccJ25 (Y9F) (supplementary data Figure 1S). The oxidation peak current at about 1.3 V is due to the oxidation of the peptides. No reduction process was observed in the reverse scan. In the oxidation process, the peak potential value (*E*p) shifts to more positive values as the sweep rate increases. Fig. 2 shows the *E*p values as a function of the logarithmic of the sweep rate (log *v*). At high sweep rates, *E*p increases linearly with log *v* as expected for an irreversible electrochemical process. At intermediate sweep rates, the dependency of *E*p with log *v* decreases, as expected for a quasi-reversible electrochemical process. At infinitely low sweep rates (reversible electrochemical process), the anodic peak potential value should be constant and lower to the half wave potential in 28.5 mV (at 25 °C for a one-electron redox process), being the half wave potential close to the formal potential [20]. Fig. 2 shows that the peak potential values for both peptides approaches to a plateau value lower than 1.1 V as the sweep rate approaches to zero. Therefore, the formal redox potential of the peptides should be lower than 1.1 V for both peptides. According to bibliography, the amino acids that present redox activity are tyrosine, glycine, cysteine and tryptophan [21,22]. From all these, MccJ25 contains 2 tyrosines and 6 glycines. The reported standard redox potential for glycine is 1.2 V [22] while for tyrosine is 0.95 V [22,23] (arrows in Fig. 2). From these we can conclude that, unless there are

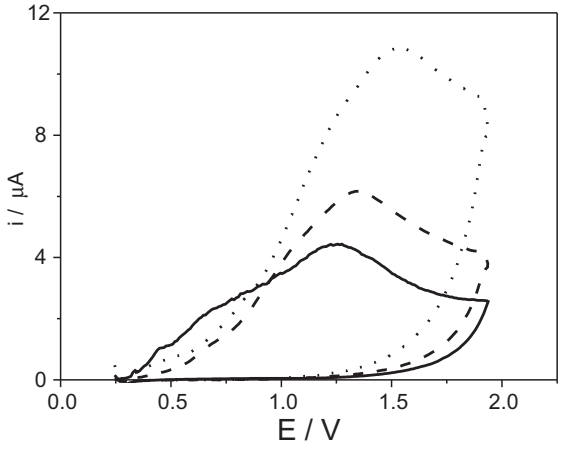

Fig. 1. Cyclic voltammogram profiles for 20 μM MccJ25 in 50 mM buffer phosphate pH 7 at 100 mV s^{-1} (solid line), 300 mV s^{-1} (dashed line), 600 mV s^{-1} (dotted line). All potentials are referred to the standard hydrogen potential. A.

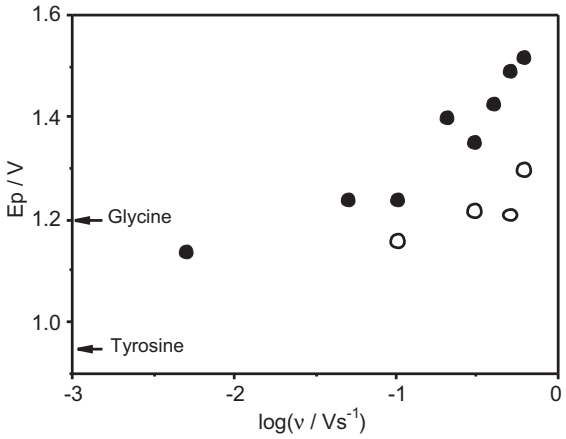

Fig. 2. Variation of the peak potential value with the logarithm of the sweep rate for MccJ25 (filled symbols) and MccJ25 (Y9F) (open symbols). All potentials are referred to the standard hydrogen potential. The arrows indicate the standard redox potential for tyrosine and glycine as reported in bibliography [22,23].

potential shifts due to the amino-acid environment, the irreversible oxidation processes observed in Fig. 1 are due to the reaction of tyrosines.

Both tyrosines (9 and 20) were oxidized on the mercury electrode, since the mutant MccJ25 (Y9F) also presented a similar oxidation peak (see supplementary data Figure 1S). The peak potential values are slightly lower for MccJ25 (Y9F) than for MccJ25 at the same scan rate, which implies that the oxidation potential of the tyrosines are different or the charge transfer process is slower for tyrosine 20 than tyrosine 9.

No quantification of the peak currents could be performed since the peptides (or the oxidation products) were absorbed on the electrode and the peak current reached a plateau value when the peptide concentration in the sample is increased due to the blocking of the electrode. The second cycle with the same mercury drop did not show faradaic current but only capacitance current (data not shown). The same behavior was observed using glassy carbon as electrode material.

The absorption process and the blocking of the electrode with each peptide are not necessarily comparable and thus, we cannot perform a qualitative comparison between the peak currents for both peptides. However, the presence of an oxidation process in MccJ25 (Y9F) is direct evidence that the oxidation of Tyr20 on the electrode occurs. Since our final proposal is to relate the MccJ25 redox capacity with its action on target membrane, this was an unexpected result taking in account that only the Tyr9 was associated with this antibiotic effect. Moreover, from the peptide structure it is clear that Tyr9 and Tyr20 have different solvent accessibility; since Tyr20 forms hydrophobic patches with the Val6 side chain and the methylene groups of the Glu8 side chain [8], while Tyr9 could be sufficiently exposed to the solvent to allow it to participate in any chemical reaction. This structural consideration led us to suggest that only the Tyr9 could be exposed to act on membrane target. Therefore, one likely explanation for the Tyr20 oxidation could be that, since the peptide adsorbs on the electrode, the secondary structure of MccJ25 could be different from that on bulk, exposing the Tyr20 residue which is not accessible when the peptide is in solution. With this in mind, we analyzed the redox reaction of the MccJ25 with $K_3Fe(CN)_6$ in homogeneous phase.

3.2. Effect of ferricyanide on the tyrosine vibration of the peptides

The sidechain of tyrosine may take part in proton and electron transfer reactions [24,25]. Tyrosine deprotonation have been involved in some redox process [26]. Moreover, the oxidized tyrosine is believed to be deprotonated [27] and thus, the effect of an oxidant substance like ferricyanide on the protonation state of tyrosine could give some insights about the redox state of the residue. In fact, it was previously reported that the one-electron oxidation of L-tyrosine by ferricyanide occurs in proteins generating the long-lived tyrosyl radical [28,29].

Considering that tyrosine is a relatively strong infrared absorber with bands sensible to changes in the protonation state, an infrared spectra analysis of MccJ25 and MccJ25 (Y9F) was performed in the absence and in the presence of ferricyanide. The results indicate that the band located around 1515 cm^{-1}, which arises from the aromatic ring (ν C–C), showed small but reproducible changes. In fact, this band can be used as marker band for the protonation state of Tyr, since it is downshifted in the deprotonated state [30]. The tyrosine wave number of MccJ25 peptide in D_2O solution shows its maximum at 1514 cm^{-1}, shifting to 1512 cm^{-1} in the presence of potassium ferricyanide. On the contrary, MccJ25 (Y9F) does not change the Tyr maximum position from 1514 cm^{-1} in the presence of ferricyanide (supplementary data Figure 2S).

In order to increase the spectral resolution and make the differences more consistent, 2D hetero-spectral correlation analysis of the normalized spectra of MccJ25 and MccJ25 (Y9F) in the presence and in the absence of ferricyanide was performed according to Schulze et al. [31]. Although the original concept of a signal involves measurements as a function of time, this term has been generalized to include measurements along other dimensions, e.g., wavenumber [32]. In fact, in the presence of ferricianyde as external perturbation, the spectroscopical response was studied by correlation analysis. Fig. 3 shows only one relevant autopeak around 1510–1518 cm^{-1}, produced by a 10^{-3} absorbance unites between the spectra of MccJ25 with and without the external perturbation. However, the correlation analysis of MccJ25 (Y9F) does not reveal any relevant autopeak in the diagonal at 10^{-3} and 10^{-6} absorbance units (data not shown). This correlation analysis support the previous 1D spectra observations. These results indicate that in

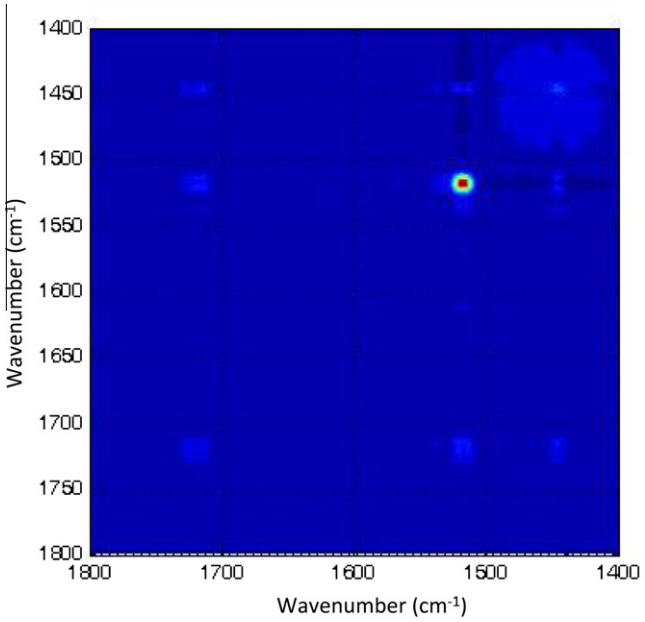

Fig. 3. 2D hetero-spectral correlation analysis of the normalized spectra of MccJ25. Synchronous 2D hetero-spectral correlation map contour in the 1800–1400 cm^{-1} interval of 2.4 mM MccJ25. The spectra were normalized and fluctuations induced by the redox reaction are in the main diagonal. The observed signals are depicted at 10^{-3} absorbance units. IR spectra were performed with and without 0.3 M of potassium ferricyanide as the perturbing agent.

homogeneous phase, the presence of ferricyanide can induce spectral changes on the Tyr9 but not on Tyr20. It is also possible to suggest that, under conditions in which cyclic voltammetry experiments were conducted; tyrosine at position 20 becomes available to be oxidized. Although MccJ25 structure is extremely stable [4,33], it is not possible to ensure that the peptide's structure is preserved intact when it is adsorbed at a mercury electrode and exposed to potential. This aspect is currently under study.

Electrochemical oxidation of Tyr is well-known to be a complex process that leads to the formation of a high-reactive tyrosyl radical [34]. The oxidized form of Tyr can be identified by its characteristic EPR signal [35,36]. The *g* value of this signal has been used to argue that the oxidation of the phenol ring is accompanied by deprotonation of the phenol OH group, giving rise to the neutral tyrosine radical [37]. This could be the case of MccJ25 tyrosine residue and would explain, therefore, the absence of a reduction peak in the above showed cathode potential sweep (Fig. 1). In this context, it is expected that once the radical is formed in the forward scan, it reacts to form a more stable species and thus, would not be available for its reduction in the backward scan.

All this led us to investigate the tyrosyl radical formation as a consequence of an oxidation process in the MccJ25 molecule.

3.3. Detection of the tyrosyl radical in MccJ25 by EPR

Globin centered radical formation in the reaction between ferric hemeproteins such as metmyoglobin (metMb) and hydrogen peroxide has been studied for 40 years. One of the free radicals from sperm whale myoglobin and hydrogen peroxide has been assigned to a tyrosyl radical through difference spectroscopy between myoglobins from different species and spin trapping experiments [38]. Experiments with site-directed mutant myoglobins implicated the Tyr-103, and not the Tyr-146, as the radical site [39].

We decided to examine whether MccJ25 was able to form a tyrosyl radical in the presence of hydrogen peroxide using EPR techniques. To assign the radical spin trapping experiments with DBNBS were performed.

The assay was performed incubating 2.4 mM MccJ25 in the presence of 2.5 mM H_2O_2 and 1 mM DBNBS (tyrosyl radical trapping). Myoglobin was used as a positive control of the reaction. Fig. 4B shows that the oxidation of MccJ25 with H_2O_2 gave rise to an EPR signal with a line shape similar to those previously reported for tyrosyl radical [39]. A control in absence of DBNBS was also performed and no signal was detected (data not shown). Moreover, to confirm that the Tyr9 of the MccJ25 was the only tyrosine involved in tyrosyl radical formation we carried out the reaction with a MccJ25 (Y9F) mutant peptide. Fig. 4C shows that the characteristic adduct signal disappeared when the reaction was made with the mutant peptide MccJ25 (Y9F). The positive control using myoglobin showed the same characteristic signal for tyrosyl radical [39] validating the result obtained for MccJ25 (Fig. 4D). These results confirmed that the Tyr9 of the MccJ25 molecule was oxidized by hydrogen peroxide generating a tyrosyl radical.

In this paper we report that the Tyr9 of the MccJ25 molecule is a redox-active tyrosine. We demonstrated by EPR experiments the tyrosyl radical presence when the MccJ25 was incubated with hydrogen peroxide and DBNBS. The adduct was absent when the experiment was conducted with de MccJ25 (Y9F) mutant indicating that the Tyr20 is not capable to give the radical. The last is in concordance with the results obtained in the redox reaction of the MccJ25 with $K_3Fe(CN)_6$ in homogeneous phase, suggesting that the Tyr9 but not Tyr20 is implicated in redox process in this condition.

We previously demonstrated that Tyr9 of MccJ25 molecule is the only amino acid involved in the membrane target action of this antibiotic [17]. In this action MccJ25 may be capable of producing radicals directly or indirectly by an intermediary in the respiratory chain that is able to generate superoxide radicals. The exact mechanism of superoxide generation by MccJ25 is currently under investigation by our group. Taking into account the results obtained in this work, we are tempted to hypothesize that this action would depend on the formation of a tyrosyl radical in the Tyr9 which would operate as an active-redox amino acid. Then, the oxidative formation of a tyrosyl radical could be connected to the proposed biological function of MccJ25 to overproduce superoxide, a reaction that could occur via reduction of dioxygen. On other hand, the MccJ25 (Y9F) mutant was able to inhibit RNAP but did not affect cellular respiration and superoxide production in an *E. coli* strain [17]. These data support the hypothesis that exist a specific mechanism of superoxide generation, probably mediated by a tyrosyl radical formation in MccJ25 molecule, rather than a general mechanism in response to the action of the antibiotic on transcription. If this is confirmed, it would be the first example of peptide antibiotics with a redox-action mechanism.

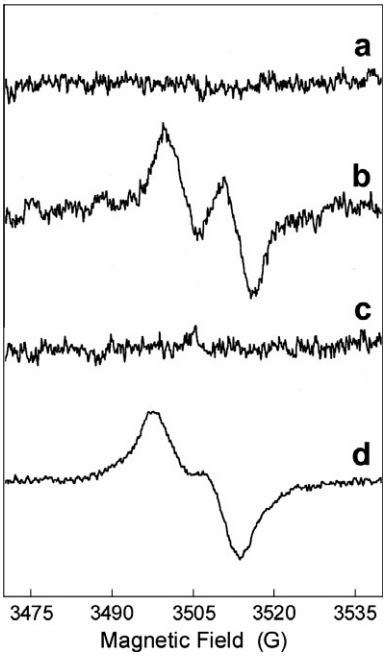

Fig. 4. EPR spectra of the tyrosyl radical generated by H_2O_2 with DBNBS in 50 mM buffer borate pH 10 (A) without peptide (baseline) or containing (B) 2.4 mM MccJ25, (C) 2.4 mM MccJ25 (Y9F), and (D) 2.4 mM myoglobin (control).

Acknowledgment

This work was funded by Grants PICT 2107 and PICTO 843 from The Agencia Nacional de Promoción Científica y Tecnológica (ANPCyT). M. C. CH. and L. C. were recipient of a fellowship from CONICET. R.D.M, R.N.F., R.N.CH., N.W and P.A.V. are Career Investigators from CONICET.

Appendix A. Supplementary data

Supplementary data associated with this article can be found, in the online version, at doi:10.1016/j.bbrc.2011.02.047.

References

[1] I. Pujols-Ayala, B.A. Barry, Tyrosyl radicals in photosystem II, Biochim. Biophys. Acta 1655 (2004) 205–216.

[2] B.A. Barry, O. Einarsdottir, Insights into the structure and function of redox-active tyrosines from model compounds, J. Phys. Chem. B 109 (2005) 6972–6981.
[3] I.R. Vassiliev, A.R. Offenbacher, B.A. Barry, Redox-active tyrosine residues in pentapeptides, J. Phys. Chem. B 109 (2005) 23077–23085.
[4] R.A. Salomon, R.N. Farias, Microcin, 25 A novel antimicrobial peptide produced by Escherichia coli, J. Bacteriol. 174 (1992) 7428–7435.
[5] S. Sable, A.M. Pons, S. Gendron-Gaillard, G. Cottenceau, Antibacterial activity evaluation of microcin J25 against diarrheagenic Escherichia coli, Appl. Environ. Microbiol. 66 (2000) 4595–4597.
[6] V. Portrait, S. Gendron-Gaillard, G. Cottenceau, A.M. Pons, Inhibition of pathogenic Salmonella enteritidis growth mediated by *Escherichia coli* microcin J25 producing strains, Can. J. Microbiol. 45 (1999) 988–994.
[7] M.J. Bayro, J. Mukhopadhyay, G.V. Swapna, J.Y. Huang, L.C. Ma, E. Sineva, P.E. Dawson, G.T. Montelione, R.H. Ebright, Structure of antibacterial peptide microcin J25: a 21-residue lariat protoknot, J. Am. Chem. Soc. 125 (2003) 12382–12383.
[8] K.J. Rosengren, R.J. Clark, N.L. Daly, U. Goransson, A. Jones, D.J. Craik, Microcin J25 has a threaded sidechain-to-backbone ring structure and not a head-to-tail cyclized backbone, J. Am. Chem. Soc. 125 (2003) 12464–12474.
[9] K.A. Wilson, M. Kalkum, J. Ottesen, J. Yuzenkova, B.T. Chait, R. Landick, T. Muir, K. Severinov, S.A. Darst, Structure of microcin J25, a peptide inhibitor of bacterial RNA polymerase, is a lassoed tail, J. Am. Chem. Soc. 125 (2003) 12475–12483.
[10] M.A. Delgado, M.R. Rintoul, R.N. Farias, R.A. Salomon, *Escherichia coli* RNA polymerase is the target of the cyclopeptide antibiotic microcin J25, J. Bacteriol. 183 (2001) 4543–4550.
[11] K. Adelman, J. Yuzenkova, A. La Porta, N. Zenkin, J. Lee, J.T. Lis, S. Borukhov, M.D. Wang, K. Severinov, Molecular mechanism of transcription inhibition by peptide antibiotic Microcin J25, Mol. Cell 14 (2004) 753–762.
[12] J. Yuzenkova, M. Delgado, S. Nechaev, D. Savalia, V. Epshtein, I. Artsimovitch, R.A. Mooney, R. Landick, R.N. Farias, R. Salomon, K. Severinov, Mutations of bacterial RNA polymerase leading to resistance to microcin j25, J. Biol. Chem. 277 (2002) 50867–50875.
[13] J. Mukhopadhyay, E. Sineva, J. Knight, R.M. Levy, R.H. Ebright, Antibacterial peptide microcin J25 inhibits transcription by binding within and obstructing the RNA polymerase secondary channel, Mol. Cell 14 (2004) 739–751.
[14] M.R. Rintoul, B.F. de Arcuri, R.A. Salomon, R.N. Farias, R.D. Morero, The antibacterial action of microcin J25: evidence for disruption of cytoplasmic membrane energization in Salmonella newport, FEMS Microbiol. Lett. 204 (2001) 265–270.
[15] P.A. Vincent, M.A. Delgado, R.N. Farias, R.A. Salomon, Inhibition of Salmonella enterica serovars by microcin J25, FEMS Microbiol. Lett. 236 (2004) 103–107.
[16] A. Bellomio, P.A. Vincent, B.F. de Arcuri, R.N. Farias, R.D. Morero, Microcin J25 has dual and independent mechanisms of action in Escherichia coli: RNA polymerase inhibition and increased superoxide production, J. Bacteriol. 189 (2007) 4180–4186.
[17] M.C. Chalon, A. Bellomio, J.O. Solbiati, R.D. Morero, R.N. Farias, P.A. Vincent, Tyrosine 9 is the key amino acid in microcin J25 superoxide overproduction, FEMS Microbiol. Lett. 300 (2009) 90–96.
[18] H. Gaussier, H. Morency, M.C. Lavoie, M. Subirade, Replacement of trifluoroacetic acid with HCl in the hydrophobic purification steps of pediocin PA-1: a structural effect, Appl. Environ. Microbiol. 68 (2002) 4803–4808.
[19] J. Turnay, N. Olmo, M. Gasset, I. Iloro, J.L. Arrondo, M.A. Lizarbe, Calcium-dependent conformational rearrangements and protein stability in chicken annexin A5, Biophys. J. 83 (2002) 2280–2291.
[20] A.J. Bard, L.R. Faulkner, Electrochemical Methods. Fundamental and Applications, New York, 2001.
[21] C.W. Hoganson, C. Tommos, The function and characteristics of tyrosyl radical cofactors, Biochim. Biophys. Acta 1655 (2004) 116–122.
[22] J. Stubbe, W.A. van Der Donk, Protein radicals in enzyme catalysis, Chem. Rev. 98 (1998) 2661–2662.
[23] M.R. DeFelippis, C.P. Murthy, M. Faraggi, M.H. Klapper, Pulse radiolytic measurement of redox potentials: the tyrosine and tryptophan radicals, Biochemistry 28 (1989) 4847–4853.
[24] G. Dollinger, L. Eisenstein, S.L. Lin, K. Nakanishi, J. Termini, Fourier transform infrared difference spectroscopy of bacteriorhodopsin and its photoproducts regenerated with deuterated tyrosine, Biochemistry 25 (1986) 6524–6533.
[25] K.J. Rothschild, Y.W. He, D. Gray, P.D. Roepe, S.L. Pelletier, R.S. Brown, J. Herzfeld, Fourier transform infrared evidence for proline structural changes during the bacteriorhodopsin photocycle, Proc. Natl. Acad. Sci. USA 86 (1989) 9832–9835.
[26] G.F. Moore, M. Hambourger, G. Kodis, W. Michl, D. Gust, T.A. Moore, A.L. Moore, Effects of Protonation State on a Tyrosine-Histidine Bioinspired Redox Mediator (dagger), J. Phys. Chem. B (2010).
[27] G. Backes, M. Sahlin, B.M. Sjoberg, T.M. Loehr, J. Sanders-Loehr, Resonance Raman spectroscopy of ribonucleotide reductase. Evidence for a deprotonated tyrosyl radical and photochemistry of the binuclear iron center, Biochemistry 28 (1989) 1923–1929.
[28] G.M. MacDonald, B.A. Barry, Difference FT-IR study of a novel biochemical preparation of photosystem II, Biochemistry 31 (1992) 9848–9856.
[29] R.C. Sealy, L. Harman, P.R. West, R.P. Mason, J. Am. Chem. Soc. 107 (1985) 3401–3406.
[30] A. Barth, The infrared absorption of amino acid side chains, Prog. Biophys. Mol. Biol. 74 (2000) 141–173.
[31] G. Schulze, A. Jirasek, M.W. Blades, R.F. Turner, Identification and interpretation of generalized two-dimensional correlation spectroscopy features through decomposition of the perturbation domain, Appl. Spectrosc. 57 (2003) 1561–1574.
[32] R.B. Panerai, A. Ambrosini, C. Bortolotti, N. D'Amico, G. Grueff, S. Mariotti, S. Montebugnoli, A. Orfei, G. Tomassetti, Spectrum Analysis and Correlation, CRC Press, LLC, 2000.
[33] A. Blond, M. Cheminant, D. Destoumieux-Garzon, I. Segalas-Milazzo, J. Peduzzi, C. Goulard, S. Rebuffat, Thermolysin-linearized microcin J25 retains the structured core of the native macrocyclic peptide and displays antimicrobial activity, Eur. J. Biochem. 269 (2002) 6212–6222.
[34] M. Voicescu, Y. El Khoury, D. Martel, M. Heinrich, P. Hellwig, Spectroscopic analysis of tyrosine derivatives: on the role of the tyrosine-histidine covalent linkage in cytochrome c oxidase, J. Phys. Chem. B 113 (2009) 13429–13436.
[35] G.T. Babcock, K. Sauer, The rapid component of electron paramagnetic resonance signal II: a candidate for the physiological donor to photosystem II in spinach chloroplasts, Biochim. Biophys. Acta 376 (1975) 329–344.
[36] C.W. Hoganson, G.T. Babcock, Protein-tyrosyl radical interactions in photosystem II studied by electron spin resonance and electron nuclear double resonance spectroscopy: comparison with ribonucleotide reductase and in vitro tyrosine, Biochemistry 31 (1992) 11874–11880.
[37] B.A. Barry, G.T. Babcock, Tyrosine radicals are involved in the photosynthetic oxygen-evolving system, Proc. Natl. Acad. Sci. USA 84 (1987) 7099–7103.
[38] M.R. Gunther, R.A. Tschirret-Guth, H.E. Witkowska, Y.C. Fann, D.P. Barr, P.R. Ortiz De Montellano, R.P. Mason, Site-specific spin trapping of tyrosine radicals in the oxidation of metmyoglobin by hydrogen peroxide, Biochem. J. 330 (Pt 3) (1998) 1293–1299.
[39] M.R. Gunther, B.E. Sturgeon, R.P. Mason, A long-lived tyrosyl radical from the reaction between horse metmyoglobin and hydrogen peroxide, Free Radic. Biol. Med. 28 (2000) 709–719.